Supporting information

Monitoring Lipid Alterations in *Drosophila* Heads in an Amyotrophic Lateral Sclerosis Model with Time-of-Flight Secondary Ion Mass Spectrometry

Minh Uyen Thi Le,[a,b,†] Jeong Hyang Park,[c,†] Jin Gyeong Son,[a,†] Hyun Kyung Shon,[a] Sunho Joh,[a] Chang Geon Chung,[c] Jae Ho Cho,[c] Alexander Pirkl,[d] Sung Bae Lee,[c,*] Tae Geol Lee[a,b*]

[a]Bio-imaging Team, Safety Measurement Institute, Korea Research Institute of Standard and Science (KRISS), Daejeon 34113, Republic of Korea
[b]Department of Nano Science, University of Science and Technology (UST), Daejeon 34113, South Korea
[c]Department of Brain Sciences, DGIST, Daegu 42988, Republic of Korea
[d]IonTOF Technologies GmbH, Helsenbergstrasse 15, 48149 Münster, Germany

†These authors contributed equally.

E-mail address reprint requests to tglee@kriss.re.kr, sblee@dgist.ac.kr.

Contents:

[SUPPEMENTARY FIGURES]

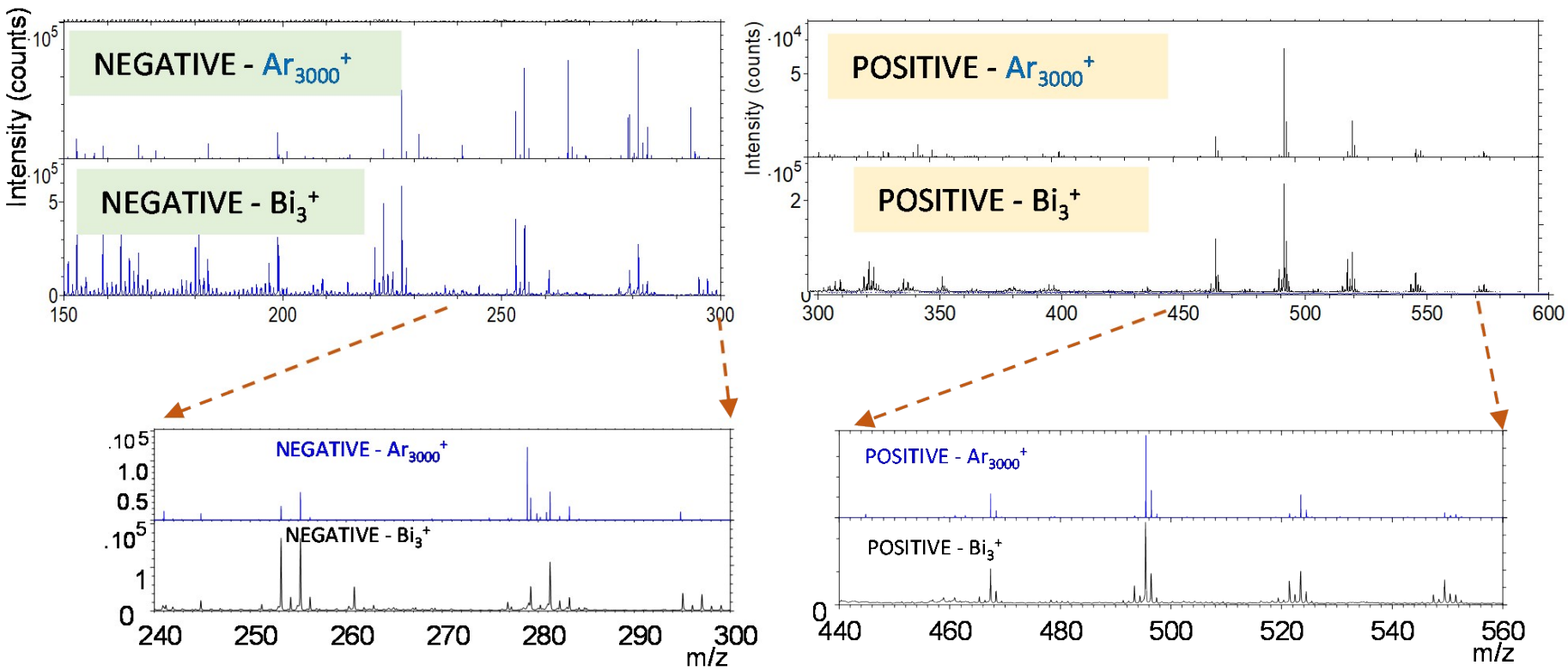

Figure S1. ToF-SIMS spectra comparison between Bi_3^+ and Ar_{3000}^+ at the low mass range in ALS fly models.

A

	Regulators	Human homologue	Fly homologue	Stock number
Biosynthesis	Acetyl-CoA carboxylase (ACC)	*ACACA*	CG11198	34885
	Sterol regulatory element binding protein (SREBP)	*SREBF2*	CG8522	25975
	ChREBP (Mondo)	*MLXIP*	CG18362	27059
Biosynthesis of phosphatidic acid and DAG	Glycerol-3-phosphate 1-O-acyltransferase (GPAT)	*GPAT3*	CG15450	61335
	CDP-diacylglycerol synthase (CDS)	*CDS1*	CG7962	58118
Uptake, activation, trafficking	Fatty acid transport protein 1 (FATP1)	*SLC27A1*	CG46149	50709
	Fatty acid binding protein (FABP)	*FABP3*	CG6783	34685
	Acyl-CoA-binding protein (ACBP)	*ACBD5*	CG8814	67020
Lipolysis	PNPLA3 (dob)	*PNPLA2*	CG5560	65925
	ATGL (Bmm)	*PNPLA2*	CG5295	25926
β-oxidation	Carnitine palmitoyltransferase 2 (CPT2)	*CPT2*	CG2107	62455

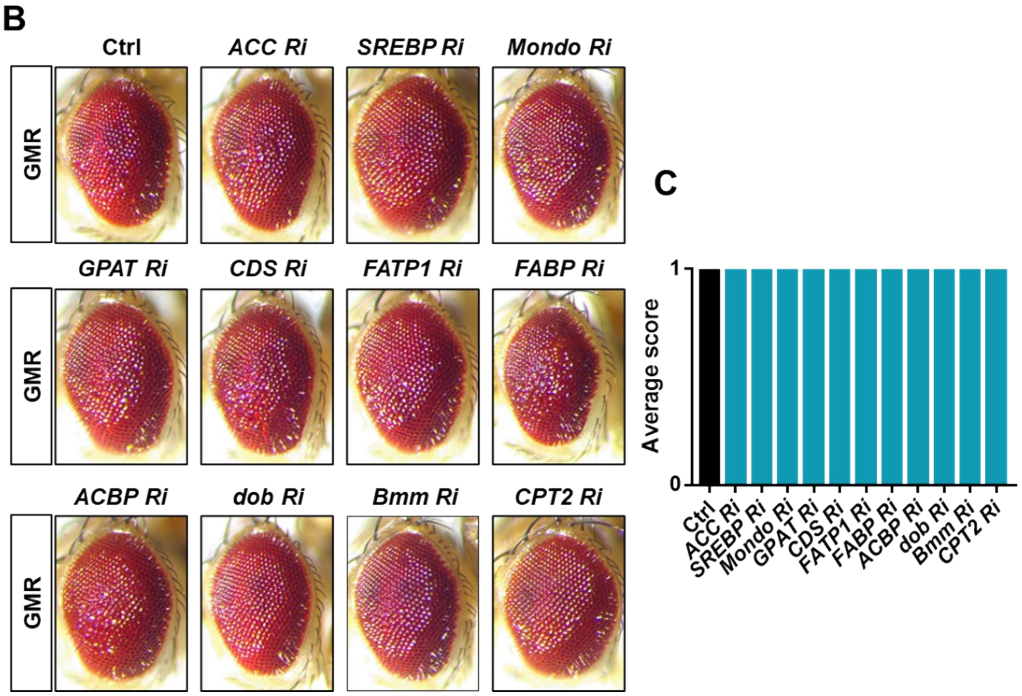

Figure S2. Screening for the lipid regulators that modify *Drosophila* eye phenotypes induced by ALS-associated $(G_4C_2)_{36}$. (A) A list of lipid regulators screened in this study. (B) Retinal images of *Drosophila* expressing the denoted RNAi (Ri) transgenes alone without $(G_4C_2)_{36}$. Fly eyes were imaged at day 1 after eclosion. (C) Quantification of the relative severity (based on the criteria shown in Figure 5B) of retinal degeneration in *Drosophila* expressing the denoted transgenes described in Supplementary Figure S3-B. n = 5 eyes. [Genotype: Ctrl, *+/+; UAS-luciferase/GMR-gal4*, *ACC Ri, +/+; UAS-ACC RNAi/ GMR-gal4, SREBP Ri, +/+; UAS-SREBP RNAi/GMR-gal4, mondo Ri, +/UAS-mondo RNAi; GMR-gal4/+, GPAT Ri, +/UAS-GPAT RNAi; GMR-gal4/+, CDS Ri, +/UAS-CDS RNAi; GMR-gal4/+, FATP1 Ri, +/+; UAS-FATP1 RNAi/GMR-gal4, FABP Ri, +/+; UAS-FABP RNAi/GMR-gal4, dob Ri, +/UAS-dob RNAi; GMR-gal4/+, bmm Ri, +/+; UAS-bmm RNAi/GMR-gal4, CPT2 Ri, +/UAS-CDS RNAi; GMR-gal4/+*].

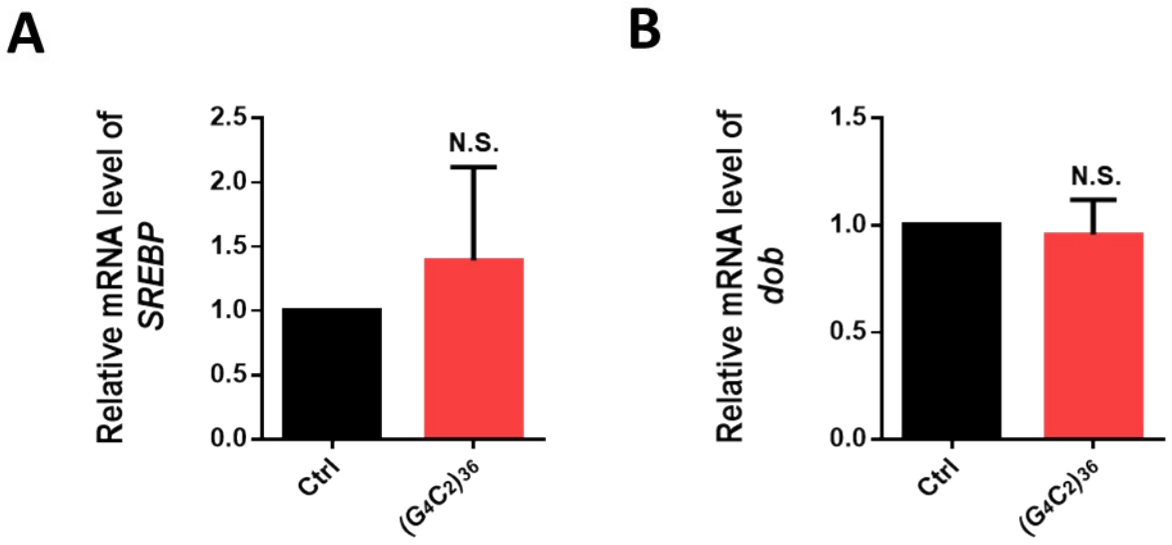

Figure S3. Quantification of mRNA levels of *SREBP* and *dob* genes in *Drosophila* expressing ALS-associated $(G_4C_2)_{36}$ at day 5 days after induction of $(G_4C_2)_{36}$ expression by RU486 treatment. The mRNA level of the *elav* gene was used as a control for normalization of the values in different sets of the experiment. The mRNA levels of lipid regulator genes in the control (Ctrl) were set to be 1.0, and their relative mRNA levels in heads expressing $(G_4C_2)_{36}$ are presented for comparison. *$p < 0.05$, N.S., not significant, $p > 0.05$ by two-tailed t-test; error bars ± SEM; $n \geq 3$ replicates. [Genotype: Ctrl, *+/elavGS-gal4*, ALS, $(G_4C_2)_{36}$/+; *elavGS-gal4/+*].

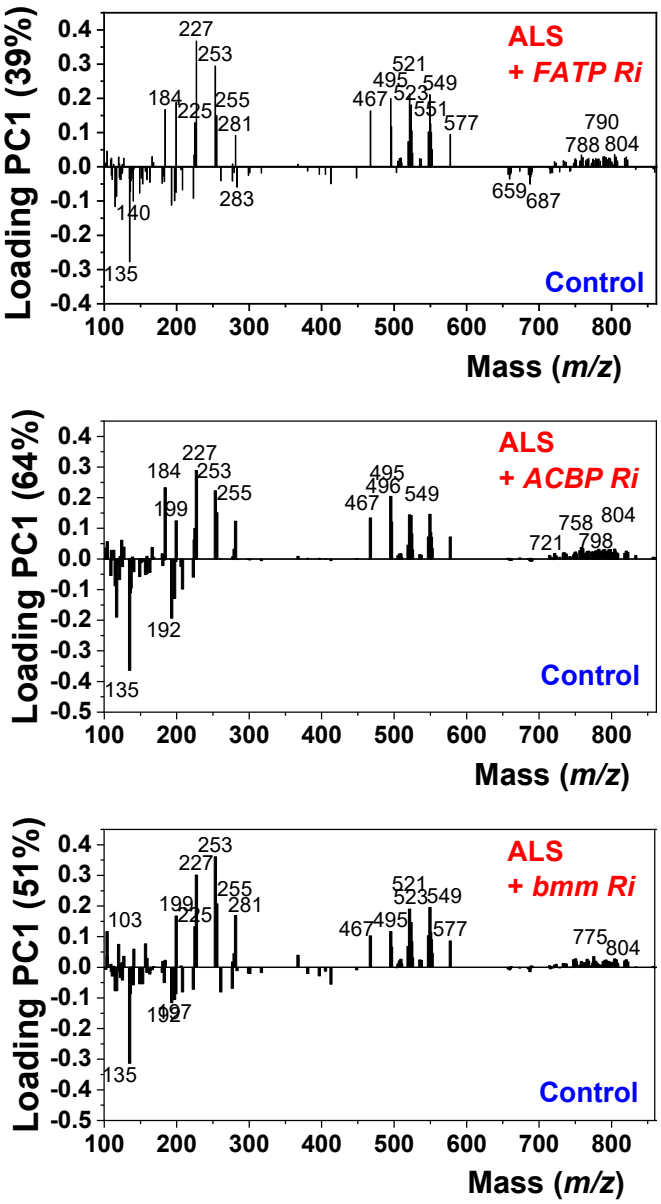

Figure S4. Loading plots of the positive and negative ions in the ToF-SIMS spectra of the indicated gene models.

[SUPPLEMENTARY TABLES]

Table S1. Summary of mass deviation of positive ions and negative ions after external calibration.

Positive Ion	Hybrid SIMS (*m/z*)	Internal Calibration (ppm)	External Calibration (ppm)
TAG(28:0)	495.440	32.30	3.03
Cer(t30:2)	496.444	32.23	3.02
TAG(32:1)	523.472	34.39	1.72
Cer(t32:3)	522.459	38.28	5.93
PC(34:2)	758.568	97.56	28.74
SHexCer(t33:1)	804.491	110.64	36.67
		57.57 (±36.34)	12.18 (±16.65)
Negative Ion	**Hybrid SIMS (*m/z*)**	**Internal Calibration (ppm)**	**External Calibration (ppm)**
FA(14:0)	227.2017	183.57	103.86
FA(16:1)	253.2174	206.98	62.79
FA(16:0)	255.2331	208.09	61.51
FA(18:1)	281.2484	244.33	41.24
		210.74 (±80.95)	67.35 (±32.21)

Table S2. Summary of the highest loading values in PC1 loading plot of the positive and negative ions in ToF-SIMS Spectra (up-regulation) between control and ALS groups

Rank	*m/z*	*PC1*	*Name*	*Formula*	*Ion*	*References*
1	227.2253	0.2484	$C_{14}H_{27}O_2$	$[M-H]^-$	FA(14:0)	[1],[2]
2	253.2333	0.204	$C_{16}H_{29}O_2$	$[M-H]^-$	FA(16:1)	[2],[3],[4],[5]
3	184.0751	0.1958	$C_5H_{15}NO_4P$	$[M+H]^+$	PC or SM fragment ion	[2],[6],[7]
4	495.4415	0.1807	$C_{31}H_{59}O4$	$[M-RCOO]^+$	TAG(28:0)	
5	255.2488	0.1594	$C_{16}H_{31}O2$	$[M-H]^-$	FA(16:0)	[2],[3],[4],[5],[8]
6	549.4888	0.1519	$C_{35}H_{65}O_4$	$[M-RCOO]^+$	TAG (32:1)	[2]
7	521.4597	0.1506	$C_{33}H_{61}O_4$	$[M-RCOO]^+$	TAG (30:1)	[2]
8	523.4711	0.1457	$C_{33}H_{63}O_4$	$[M-RCOO]^+$	TAG(30:0)	[2],[8]
9	467.4115	0.1412	$C_{29}H_{55}O_4$	$[M-RCOO]^+$	TAG(26:0)	
10	281.2603	0.1365	$C_{18}H_{33}O_2$	$[M-H]^-$	FA(18:1)	[2],[3],[5]
11	199.188	0.1279	$C_{12}H_{23}O_2$	$[M-H]^-$	FA(12:0)	[9]
12	496.4425	0.1087	$C_{30}H_{58}NO_4$	$[M+H]^+$	Cer(t30:2)	
13	104.1131	0.0964	$C_5H_{14}NO$	$[M+H]^+$	PC fragment ion	[2],[6],[7]
14	228.2274	0.0962	—	—	unknown	
15	550.4988	0.0914	$C_{36}H_{72}NO_2$	$[M+H]^+$	Cer(d36:0)	
16	522.4559	0.0909	$C_{32}H_{60}NO_4$	$[M+H]^+$	Cer(t32:3)	
17	225.2014	0.0886	$C_{14}H_{25}O_2$	$[M-H]^-$	FA(14:1)	
18	493.4186	0.0883	$C_{31}H_{57}O_4$	$[M-RCOO]^+$	TAG(28:1)	
19	279.246	0.0862	$C_{18}H_{31}O_2$	$[M-H]^-$	FA(18:2)	[2],[3],[5]
20	524.4778	0.0846	$C_{32}H_{62}NO_4$	$[M+H]^+$	Cer(t32:2)	
21	254.2368	0.0839	—	—	unknown	
22	468.4078	0.0791	$C_{32}H_{54}NO$	$[M+H-H2O]^+$	NAE(30:5)	
23	285.2434	0.0784	$C_{17}H_{33}O_3$	$[M+H-H_2O]^+$	MAG(14:0)	
24	551.5111	0.0769	$C_{35}H_{67}O_4$	$[M-RCOO]^+$	TAG (32:0)	[2],[3],[4],[8]
25	211.217	0.0739	$C_{14}H_{27}O$	$[M+H-H_2O]^+$	WE(14:0)	
26	547.4827	0.0702	$C_{35}H_{63}O_4$	$[M-RCOO]^+$	TAG (32:2)	[2]
27	577.5044	0.0701	$C_{37}H_{69}O_4$	$[M-RCOO]^+$	TAG (34:1)	[2],[3],[4]
28	256.2385	0.0626	$C_{15}H_{30}NO_2$	$[M-H]^-$	NAE(13:0)	
29	282.2604	0.0589	—	—	unknown	
30	237.211	0.0536	—	—	unknown	
31	224.1085	0.053	$C_8H_{19}PNO_4$	$[M+H]^+$	PC fragment ion	[2],[6],[7]
32	465.3821	0.048	$C_{29}H_{53}O_4$	$[M-RCOO]^+$	TAG(26:1)	
33	519.4309	0.0469	$C_{34}H_{63}O_3$	$[M-RCOO]^+$	TAG (P-31:1)	
34	140.0337	0.0461	—	—	unknown	
35	575.4696	0.0454	$C_{37}H_{67}O_4$	$[M-RCOO]^+$	TAG (O-34:4)	[2]
36	548.4719	0.0453	—	—	unknown	
37	180.0518	0.0448	—	—	unknown	
38	497.4456	0.0442	$C_{31}H_{61}O_4$	$[M+H]^+$	MAG(28:1)	
39	804.4615	0.0405	$C_{39}H_{75}NO_{12}SNa$	$[M+Na]^+$	SHexCer(t33:1)	
40	313.2738	0.0393	$C_{19}H_{37}O_3$	$[M+H-H_2O]^+$	MAG(16:0)	[2]

41	578.4665	0.0389	$C_{36}H_{68}NO_4$	$[M+H]^+$	Cer(t36:3)	
42	552.5027	0.0383	$C_{34}H_{66}NO_4$	$[M+H]^+$	Cer(t34:2)	
43	790.482	0.036	$C_{39}H_{77}NO_{11}SNa$	$[M+Na]^+$	SHexCer(d33:0)	
44	806.465	0.0356	$C_{39}H_{77}NO_{11}SK$	$[M+K]^+$	SHexCer(d33:0)	
45	280.2445	0.0356	—	—	unknown	
46	758.5462	0.0354	$C_{42}H_{81}NO_8P$	$[M+H]^+$	PC(34:2)	[2]
47	311.2637	0.0337	$C_{20}H_{39}O_2$	$[M+H]^+$	WE(20:1)	
48	283.268	0.0337	$C_{18}H_{35}O_2$	$[M-H]^-$	FA(18:0)	[2],[4],[5],[8]
49	788.4959	0.0328	$C_{43}H_{76}NO_7PK$	$[M+K]^+$	PE(P-38:5)	
50	520.4327	0.0318	—	—	unknown	
51	525.4774	0.0309	$C_{33}H_{65}O_4$	$[M-RCOO]^+$	TAG (O-30:1)	
52	277.2137	0.0307	$C_{18}H_{29}O_2$	$[M-H]^-$	FA(18:3)	[5]
53	759.5625	0.0306	$C_{49}H_{91}O_5$	$[M+H-H2O]^+$	TAG(46:1)	
54	796.4793	0.0306	$C_{42}H_{80}NO_8PK$	$[M+K]^+$	PC(34:2)	[2],[5],[10],[11]
55	760.545	0.0303	$C_{42}H_{83}NO_8P$	$[M+H]^+$	PC(34:1)	

Notes

Fatty acyls (FA); Phosphtatidylcholines (PC); Mono(acyl|alkyl)glycerols (MAG); N-acyl ethanolamines (NAE); Phosphtatidylethanolamines (PE); Sulfatides hexosyl ceramide (SHexCer); Tri(acyl|alkyl)glycerols (TAG); Phosphtatidylglycerols (PG); Ceramides (Cer); Phosphtatidylinositols(PI); Sphingomyelins (SM), Wax monoesters (WE)

Table S3. Discriminant ion list is selected by the highest contribution loading PC1 of the positive and negative ions in ToF-SIMS Spectra (up-regulation) between each modification *Drosophila* model, control and ALS groups.

Group	m/z	PC1	Formula	Ion	Name	References
ALS + FATP1 Ri	227.2	0.4198	$C_{14}H_{27}O_2$	$[M-H]^-$	FA(14:0)	[1],[2]
	253.2	0.2888	$C_{16}H_{29}O_2$	$[M-H]^-$	FA(16:1)	[2],[3],[4],[5]
	495.4	0.2305	$C_{31}H_{59}O_4$	$[M-RCOO]^+$	TAG(28:0)	
	521.4	0.218	$C_{33}H_{61}O_4$	$[M-RCOO]^+$	TAG(30:1)	[2]
	549.4	0.203	$C_{35}H_{65}O_4$	$[M-RCOO]^+$	TAG(32:1)	[2]
	199.2	0.1974	$C_{12}H_{23}O_2$	$[M-H]^-$	FA(12:0)	[9]
	523.4	0.1879	$C_{33}H_{63}O_4$	$[M-RCOO]^+$	TAG(30:0)	[2],[8]
	467.3	0.1745	$C_{29}H_{55}O_4$	$[M-RCOO]^+$	TAG(26:0)	
	184.1	0.1493	$C_5H_{15}PNO_4$	$[C_5H_{15}PNO_4]^+$	PC head group	[2],[6],[7]
	225.2	0.1406	$C_{14}H_{25}O_2$	$[M-H]^-$	FA(14:1)	
	496.4	0.136	$C_{30}H_{58}NO_4$	$[M+H]^+$	Cer(t30:2)	
	522.4	0.1291	$C_{32}H_{60}NO_4$	$[M+H]^+$	Cer(t32:3)	
	550.4	0.1218	$C_{34}H_{64}NO_4$	$[M+H]^+$	Cer(t34:3)	
	524.4	0.1096	$C_{32}H_{62}NO_4$	$[M+H]^+$	Cer(t32:2)	
	547.4	0.0981	$C_{35}H_{63}O_4$	$[M-RCOO]^+$	TAG(32:2)	[2]
	551.4	0.098	$C_{35}H_{67}O_4$	$[M-RCOO]^+$	TAG(32:0)	[2],[3],[4],[8]
	255.2	0.0926	$C_{16}H_{31}O_2$	$[M-H]^-$	FA(16:0)	[2],[3],[4],[5],[8]
	577.5	0.0837	$C_{37}H_{69}O_4$	$[M-RCOO]^+$	TAG(34:1)	[2],[3],[4]
ALS + ACBP Ri	227.2	0.3023	$C_{14}H_{27}O_2$	$[M-H]^-$	FA(14:0)	[1],[2]
	184.1	0.2392	$C_5H_{15}PNO_4$	$[C_5H_{15}PNO_4]^+$	PC head group	[2],[6],[7]
	253.2	0.2349	$C_{16}H_{29}O_2$	$[M-H]^-$	FA(16:1)	[2],[3],[4],[5]
	495.4	0.2038	$C_{31}H_{59}O_4$	$[M-RCOO]^+$	TAG(28:0)	[12]
	255.2	0.152	$C_{16}H_{31}O_2$	$[M-H]^-$	FA(16:0)	[2],[3],[4],[5],[8]
	549.4	0.1448	$C_{35}H_{65}O_4$	$[M-RCOO]^+$	TAG(32:1)	[2]
	521.4	0.1426	$C_{33}H_{61}O_4$	$[M-RCOO]^+$	TAG(30:1)	[2]
	523.4	0.1398	$C_{33}H_{63}O_4$	$[M-RCOO]^+$	TAG(30:0)	[2],[8]
	467.3	0.1271	$C_{29}H_{55}O_4$	$[M-RCOO]^+$	TAG(26:0)	
	199.2	0.125	$C_{12}H_{23}O_2$	$[M-H]^-$	FA(12:0)	[9]
	281.2	0.1214	$C_{18}H_{33}O_2$	$[M-H]^-$	FA(18:1)	[2],[3],[5]
	496.4	0.12	$C_{30}H_{58}NO_4$	$[M+H]^+$	Cer(t30:2)	
	225.2	0.104	$C_{14}H_{25}O_2$	$[M-H]^-$	FA(14:1)	
	550.4	0.0859	$C_{34}H_{64}NO_4$	$[M+H]^+$	Cer(t34:3)	
	522.4	0.0853	$C_{32}H_{60}NO_4$	$[M+H]^+$	Cer(t32:3)	
	524.4	0.0802	$C_{32}H_{62}NO_4$	$[M+H]^+$	Cer(t32:2)	
	547.4	0.0724	$C_{35}H_{63}O_4$	$[M-RCOO]^+$	TAG(32:2)	[2]

Group	m/z	PC1	Formula	Ion	Name	References
ALS + Bmm Ri	253.2	0.3932	$C_{16}H_{29}O_2$	$[M-H]^-$	FA(16:1)	
	227.2	0.2945	$C_{14}H_{27}O_2$	$[M-H]^-$	FA(14:0)	[1],[2]
	103.9	0.1978	—	—	unknown	
	255.2	0.1923	$C_{14}H_{25}O_2$	$[M-H]^-$	FA(14:1)	
	549.4	0.1768	$C_{35}H_{65}O_4$	$[M-RCOO]^+$	TAG(32:1)	[2]
	521.4	0.171	$C_{33}H_{61}O_4$	$[M-RCOO]^+$	TAG(30:1)	[2]
	199.2	0.155	$C_{12}H_{23}O_2$	$[M-H]^-$	FA(12:0)	[9]
	281.2	0.1534	$C_{18}H_{33}O_2$	$[M-H]^-$	FA(14:1)	[2],[3],[5]
	156.9	0.1524	—	—	unknown	
	225.2	0.1382	$C_{14}H_{25}O_2$	$[M-H]^-$	FA(14:1)	
	140.9	0.1296	—	—	unknown	
	119.9	0.1248	—	—	unknown	
	523.4	0.1156	$C_{33}H_{63}O_4$	$[M-RCOO]^+$	TAG(30:0)	[2],[8]
	550.4	0.1015	$C_{34}H_{64}NO_4$	$[M+H]^+$	Cer(t34:3)	
	547.4	0.0992	$C_{35}H_{63}O_4$	$[M-RCOO]^+$	TAG(32:2)	[2]
	522.4	0.0967	$C_{32}H_{60}NO_4$	$[M+H]^+$	Cer(t32:3)	
	551.4	0.078	$C_{35}H_{67}O_4$	$[M-RCOO]^+$	TAG(32:0)	[2],[3],[4],[8]
	577.5	0.0739	$C_{37}H_{69}O_4$	$[M-RCOO]^+$	TAG(34:1)	[2],[3],[4]

1. Melissa K. Passarelli and N. Winograd, *Lipid imaging with time-of-flight secondary ion mass spectrometry (ToF-SIMS).* Biochimica et Biophysica Acta, 2011. **1811**: p. 976-990.
2. Claudia Bich, David Touboul, and A. Brunelle, *Study of experimental variability in TOF-SIMS mass spectrometry imaging of biological samples.* International Journal of Mass Spectrometry, 2013. **337**: p. 43-49.
3. Per Malmberg, et al., *Imaging of Lipids in Human Adipose Tissue by Cluster Ion TOF-SIMS.* MICROSCOPY RESEARCH AND TECHNIQUE, 2007. **70**: p. 828-835.
4. Ylva Magnusson, et al., *Lipid imaging of human skeletal muscle using TOF-SIMS with bismuth cluster ion as a primary ion source.* Clin Physiol Funct Imaging, 2008. **28**: p. 202-209.
5. David Touboul, et al., *Lipid imaging by gold cluster time-of-flight secondary ion mass spectrometry: application to Duchenne muscular dystrophy.* Journal of Lipid Research, 2005. **46**: p. 1388-1395.
6. David Touboul, A. Brunelle, and O. Lapre´vote, *Structural analysis of secondary ions by post-source decay in time-of-flight secondary ion mass spectrometry.* 2006. **20**: p. 703-709.
7. Nora Tahallah, Alain Brunelle, and O.L.v. Sabine De La Porte, *Lipid mapping in human dystrophic muscle by cluster-time-of-flight secondary ion mass spectrometry imaging.* Journal of Lipid Research, 2008. **49**: p. 438-454.
8. ·, D.B.S.S.-D. and B.J.M.S.P. Sjövall, *Chemical analysis of osmium tetroxide staining in adipose tissue using imaging ToF-SIMS.* Histochem Cell Biol, 2009. **132**: p. 105-115.
9. Sanna Sämfors and J.S. Fletcher, *Lipid Diversity in Cells and Tissue Using Imaging SIMS.* nnual Rev. Anal. Chem., 2020. **13**: p. 249-271.
10. Peter Sjo1 vall, Jukka Lausmaa, and B. Johansson, *Mass Spectrometric Imaging of Lipids in Brain Tissue.* Anal. Chem., 2004. **76**: p. 4271-4278.
11. Peter Sjo¨vall and J.L. Bjo¨rn Johansson, *Localization of lipids in freeze-dried mouse brain sections by imaging TOF-SIMS.* Applied Surface Science, 2006. **252**: p. 6966-6974.
12. Phan, N.T.N., et al., *MS/MS analysis and imaging of lipids across Drosophila brain using secondary ion mass spectrometry.* Anal Bioanal Chem, 2017. **409**(16): p. 3923-3932.